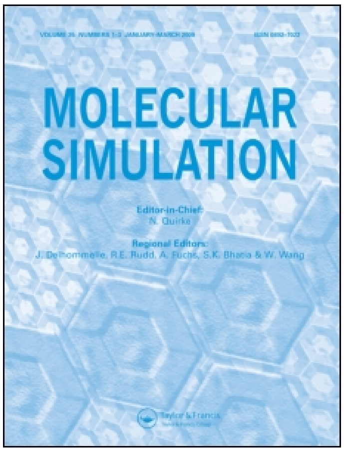

Molecular Simulation
Publication details, including instructions for authors and subscription information:
http://www.informaworld.com/smpp/title~content=t713644482

An analytical subthreshold current model for ballistic quantum-wire double-gate MOS transistors

J. L. Autran[a]; D. Munteanu[a]; O. Tintori[a]; E. Decarre[a]; A. M. Ionescu[b]
[a] Laboratory for Materials and Microelectronics of Provence (L2MP, UMR CNRS 6137) Bâtiment IRPHE, Marseille Cedex 13, France [b] Electronics Laboratories (LEG), Swiss Federal Institute of Technology Lausanne, Lausanne, Switzerland

To cite this Article Autran, J. L. , Munteanu, D. , Tintori, O. , Decarre, E. and Ionescu, A. M.(2005) 'An analytical subthreshold current model for ballistic quantum-wire double-gate MOS transistors', Molecular Simulation, 31: 2, 179 — 183

To link to this Article: DOI: 10.1080/0892702051233132

URL: http://dx.doi.org/10.1080/0892702051233132

Molecular Simulation, Vol. 31, No. 2–3, 15 February–15 March 2005, 179–183

Taylor & Francis
Taylor & Francis Group

An analytical subthreshold current model for ballistic quantum-wire double-gate MOS transistors

J.L. AUTRAN*†¶, D. MUNTEANU†, O. TINTORI†, E. DECARRE† and A.M. IONESCU‡

†Laboratory for Materials and Microelectronics of Provence (L2MP, UMR CNRS 6137) Bâtiment IRPHE, 49 rue Joliot-Curie, BP 146, F-13384 Marseille Cedex 13, France
‡Electronics Laboratories (LEG), Swiss Federal Institute of Technology Lausanne, CH-1015 Lausanne, Switzerland

(Received April 2004; in final form October 2004)

The subthreshold characteristic of ultra-thin (i.e. quantum-wire), ultra-short double-gate transistors (symmetric structures) working in the ballistic regime has been analytically modeled. This model takes into account short-channel effects, quantization effects and source-to-drain tunneling (WKB approximation) in the expression of the subthreshold drain current. Important device parameters, such as I_{off}-current or subthreshold swing, can be easily evaluated through this full analytical approach, which also provides a complete set of equations for developing equivalent-circuit model used in ICs simulation.

Keywords: Ballistic transport; Double-gate devices; Analytical modeling; Subthreshold current model

Introduction

Double-gate (DG) MOSFETs are extensively investigated because of their promising performances with respect to the ITRS specifications for decananometer channel lengths. One of the identified challenges remains the development of compact models [1–3] taking into account the main physical phenomena governing the devices at this scale of integration. In this work, an analytical subthreshold model of ultra-thin DG MOSFETs working in the ballistic regime is presented. As we show in the following, the present approach captures the essential physics of such ultimate DG devices (quantum confinement, thermionic current) and introduces two main novelties usually neglected in compact modeling: the 2D short-channel effects and the tunneling of carriers through the source-to-drain barrier. Results given by this analytical approach are finally compared with data obtained with a full-2D numerical code coupling the Schrödinger–Poisson system with the ballistic transport equation.

Modeling of the ballistic subthreshold current

Figure 1 shows the schematic n-channel DG structure with symmetric gates considered in this work. Carrier transport in the ultra-thin silicon film (thickness t_{Si}, doping level N_{A}) is clearly 1D in the x-direction and the resulting current is controlled by the gate-to-source (V_{GS}) and drain-to-source (V_{DS}) voltages which impact the shape as well as the amplitude of the source-to-drain energy barrier. In the subthreshold regime, minority carriers can be neglected and Poisson's equation is analytically solved in the x-direction with explicit boundary conditions at the two oxide/silicon interfaces taking into account the electrostatic influence of V_{GS}. Considering the particular closed surface shown in figure 1 for Gauss's law integration, we can write:

$$-\xi(x)\frac{t_{\mathrm{Si}}}{2}+\xi(x+\mathrm{d}x)\frac{t_{\mathrm{Si}}}{2}-\xi_{\mathrm{S}}(x)=-\frac{qN_{\mathrm{A}}t_{\mathrm{Si}}\mathrm{d}x}{2\varepsilon_{\mathrm{Si}}} \qquad (1)$$

where the electric field $\xi(x)\approx -\mathrm{d}\psi(x)/\mathrm{d}x$ (due to the 1D character of the electrostatic potential (ψ in the Silicon film) and $\xi_{\mathrm{S}}(x)=\frac{\varepsilon_{\mathrm{ox}}}{\varepsilon_{\mathrm{Si}}}\xi_{\mathrm{ox}}(x)$.

Defining the electrostatic potential ψ as the band bending with respect to the intrinsic Fermi level in the Silicon film and choosing the Fermi level in the source reservoir as the potential reference, the oxide electric field $\xi_{\mathrm{ox}}(x)$ along the structure is then given by:

$$\xi_{\mathrm{ox}}(x)=\frac{V_{\mathrm{GS}}-V_{\mathrm{FB}}-\psi(x)-\phi_{\mathrm{F}}}{t_{\mathrm{ox}}} \qquad (2)$$

*Corresponding author. Tel.: +33-4-96-13-97-17. Fax: +33-4-96-13-97-09. E-mail: autran@newsup.univ-mrs.fr
¶(also with Institut Universitaire de France)

Molecular Simulation
ISSN 0892-7022 print/ISSN 1029-0435 online © 2005 Taylor & Francis Group Ltd
http://www.tandf.co.uk/journals
DOI: 10.1080/0892702051233132

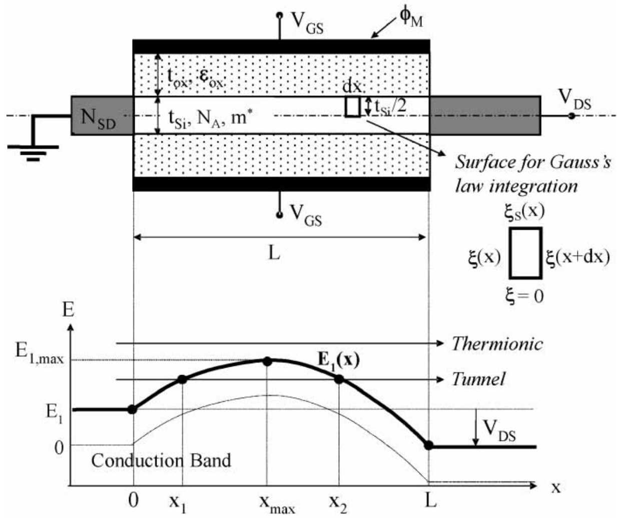

Figure 1. Schematic ultra-thin DG structure and its technological and electrical parameters considered in this work. The first energy subband profile $E_1(x)$ obtained from equation (11) is also represented. Turning points (x_1, x_2) and $x_{\max}$ have literal values due to the analytical character of $E_1(x)$.

where $V_{\rm FB}$ is the flat-band voltage and $\phi_{\rm F}$ is the bulk potential of the Silicon film.

After some algebraic manipulations, we obtained the following differential equation for the electrostatic potential in the Silicon film:

$$\frac{\mathrm{d}^2\psi}{\mathrm{d}x^2}-\frac{2C_{\rm ox}}{\varepsilon_{\rm Si}t_{\rm Si}}\psi=\frac{1}{\varepsilon_{\rm Si}t_{\rm Si}}\left[qN_{\rm A}t_{\rm Si}-2C_{\rm ox}(V_{\rm GS}-V_{\rm FB}-\phi_{\rm F})\right] \quad (3)$$

where $C_{\rm ox}=\varepsilon_{\rm ox}/t_{\rm ox}$ is the gate capacitance per unit area.

The analytical solution of equation (3) can be then expressed under the form:

$$\psi(x) = C_1\exp(m_1x) + C_2\exp(-m_1x) - \frac{R}{m_1^2} \quad (4)$$

where the coefficients C_1 and C_2 are given by:

$$C_1 = \frac{\phi_{\rm S}[1-\exp(-m_1L)] + V_{\rm DS} + \frac{R[1-\exp(-m_1L)]}{m_1^2}}{2\sinh(m_1L)} \quad (5)$$

$$C_2 = -\frac{\phi_{\rm S}[1-\exp(+m_1L)] + V_{\rm DS} + \frac{R[1-\exp(+m_1L)]}{m_1^2}}{2\sinh(m_1L)} \quad (6)$$

with:

$$R = \frac{1}{\varepsilon_{\rm Si}t_{\rm Si}}\left[qN_{\rm A}t_{\rm Si} - 2C_{\rm ox}(V_{\rm GS}-V_{\rm FB}-\phi_{\rm F})\right] \quad (7)$$

$$m_1 = \sqrt{\frac{2C_{\rm ox}}{\varepsilon_{\rm Si}t_{\rm Si}}} \quad (8)$$

$$\phi_S = \frac{kT}{q}\ln\left(\frac{N_{\rm A}N_{\rm SD}}{n_i^2}\right) \quad (9)$$

$$\phi_{\rm F} = \frac{kT}{q}\ln\left(\frac{N_{\rm A}}{n_i}\right) \quad (10)$$

Considering the limit case of an ultra-thin Silicon film, the vertical confinement of carriers in the structure can be treated using the well-known approximation of an infinitely deep square well. The first energy subband profile $E_1(x)$ can be easily derived as:

$$E_1(x) = q\big(\phi_{\rm S} - \psi(x)\big) + \frac{\hbar^2\pi^2}{2m_\ell^* t_{\rm Si}^2} \quad (11)$$

where $m_\ell^* \approx 0.98\times m_0$ is the electron longitudinal mass.

Once $E_1(x)$ is known as a function of $V_{\rm GS}$ and $V_{\rm DS}$, the total ballistic current (per device width unit) can be evaluated as follows:

$$I_{\rm DS} = I_{\rm Therm} + I_{\rm Tun} \quad (12)$$

where $I_{\rm Term}$ and $I_{\rm Tun}$ are the thermionic and the tunneling components of the ballistic current, respectively. For a two-dimensional gas of electrons [4]:

$$I_{\rm Therm} = \frac{2q}{\pi^2\hbar}\int_{-\infty}^{+\infty}\mathrm{d}k_z \times \int_{E_{1,\max}}^{+\infty}\left[f(E,E_{\rm FS}) - f(E,E_{\rm FD})\right]\mathrm{d}E_x \quad (13)$$

$$I_{\rm Tun} = \frac{2q}{\pi^2\hbar}\int_{-\infty}^{+\infty}\mathrm{d}k_z \times \int_{E_1}^{E_{1,\max}}\left[f(E,E_{\rm FS}) - f(E,E_{\rm FD})\right]T(E_{\rm x})\,\mathrm{d}E_{\rm x} \quad (14)$$

where $f(E_{\rm F}, E_{\rm FS})$ is the Fermi–Dirac distribution function, $E_{\rm FS}$ and $E_{\rm FD}$ are the Fermi-level in the source and drain reservoirs, respectively ($E_{\rm FD} = E_{\rm FS} - qV_{\rm DS}$), k_z is the electron wave vector component in the z-direction, the factor 2 accounts for the two Silicon valleys characterized by m_ℓ^* in the y-direction (vertical confinement) and $T(E_x)$ is the barrier transparency for electrons and E is the total energy of carriers in source and drain reservoirs given by:

$$E = E_1 + E_x + \frac{\hbar^2k_z^2}{2m_{\rm t}^*} \quad (15)$$

where E_1 is the energy level of the first subband (given by equation (11)), E_x is the carrier energy in the direction of the current, $m_{\rm t}$* is the electron transverse effective mass.

In equation (14), $T(E_{\rm x})$ is evaluated considering the well-known WKB approximation [5]:

$$\begin{cases} T_{\rm WKB}(E_{\rm x} \le E_{1,\max}) = \exp\left(-2\int_{x_1}^{x_2}\sqrt{\frac{2m_{\rm t}^*(E_{\rm x}-E_1(x))}{\hbar^2}}\mathrm{d}x\right) \\ T_{\rm WKB}(E_{\rm x} > E_{1,\max}) = 1 \end{cases} \quad (16)$$

where the turning point coordinates x_1 and x_2 have literal expressions due to the analytical character of the barrier:

$$x_{1,2}(E_x) = \frac{1}{m_1} \ln \left[\frac{A \pm \sqrt{\Delta}}{2C_1} \right] \tag{17}$$

where the quantities A and Δ are defined as follows:

$$A = \phi_S + \frac{R}{m_1^2} + \frac{\hbar^2 \pi^2}{2qm_\ell^* t_{Si}^2} - \frac{E_x}{q} \tag{18}$$

$$\Delta = A^2 - 4C_1C_2 \tag{19}$$

If one remarks that the top (i.e. the maximum) of the source-to-drain barrier has an analytic character using equations (11)–(17), the thermionic component of the ballistic current can then be fully analytically derived from equation (13) using the well-known Natori's formula [1]:

$$I_{Therm} = I_0 \left[\Im_{1/2}(E_{FS} - E_1(x_{max})) - \Im_{1/2}\left(E_{FS} - E_1(x_{max}) - qV_{DS}\right) \right] \tag{20}$$

with:

$$I_0 = \frac{2q}{\hbar^2} \left(\frac{kT}{\pi} \right)^{3/2} \sqrt{2m_t^*} \tag{21}$$

$$x_{max} = \frac{1}{2m_1} \log \left(\frac{C_2}{C_1} \right) \tag{22}$$

$$\Im_{1/2}(\eta) = \int_0^{+\infty} \frac{\sqrt{y}}{1 + \exp\left(y - \eta\right)} dy \tag{23}$$

Finally, the tunneling component of the ballistic current can be evaluated from equation (14) using a simple rectangular double integration method on the energy interval $[E_1, E_{1,max}]$ (transforming the integral into discrete sums). The development of analytical approximations for this tunneling component is envisaged in a future work.

Results and model validation

Figure 2 shows the first energy subband profile $E_1(x)$ in the Silicon film calculated with the analytical model for different gate voltages in a $L = 10$ nm device. In order to test the validity of the model, we compare these profiles with those obtained with a full quantum-mechanical 2D simulation code (BALMOS [6]). A good agreement is obtained between the two series of subband profiles, especially for low V_{GS} values, i.e. in the subthreshold regime. In particular, we note an excellent agreement for the positions of the maximum as well as the amplitude of the barrier between the analytical and numerical curves. The slight difference in the barrier width is due to the electric field penetration in the source and drain regions, only taken into account in the numerical approach. Concerning this point, the analytical model should perfectly reproduce the barrier profile for devices with metallic source and drain, as in Schottky-barrier transistors recently proposed [7]. When approaching the threshold voltage (e.g. $V_{GS} = 0.1$ V), the numerical and analytical profiles diverge, due to the presence of minority carriers in the channel, which is not taken into account by the analytical model. This limitation sets the validity domain of this later approach, as illustrated in figures 3 and 4 (hatched area).

The subthreshold $I_{DS}(V_{GS})$ characteristics calculated with the analytical model for devices ranging from $L = 5$ to 20 nm are shown in figure 3. In the subthreshold regime (typically $V_{GS} < 0.1$ V), the curves very well fit numerical data obtained with BALMOS for devices in the deca-nanometer range. Below $L = 10$ nm, the effect of electric field penetration in source and drain regions on the barrier width becomes significant, leading to a slight overestimation of the drain current in the analytical case.

Figure 4 shows subthreshold $I_{DS}(V_{GS})$ characteristics calculated with the analytical model. Considering the WKB

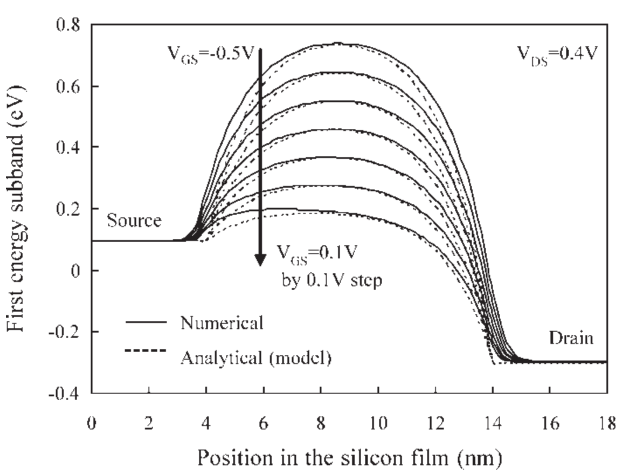

Figure 2. First energy subband profiles $E_1(x)$ in the silicon film calculated with the analytical model (equation (11)) and with the 2D numerical code BALMOS [6]. Device parameters are: $L = 10$ nm, $t_{Si} = 2$ nm, $t_{ox} = 0.8$ nm, $\phi_M = 4.3$ V, $N_{SD} = 3 \times 10^{20}$ cm^{-3}, $N_A = 10^{15}$ cm^3.

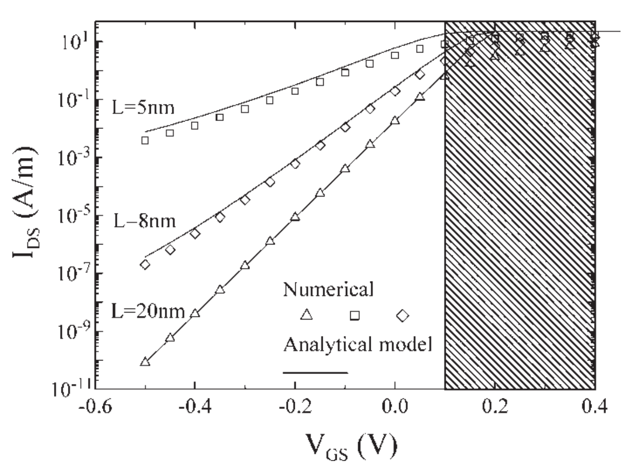

Figure 3. $I_{DS}(V_{GS})$ characteristics calculated with the analytical model. Values obtained with the 2D numerical code BALMOS [6] are also reported for comparison. The hachured area represents the near and above threshold regions where the analytical model losses its validity. Device parameters are the same as in figure 2.

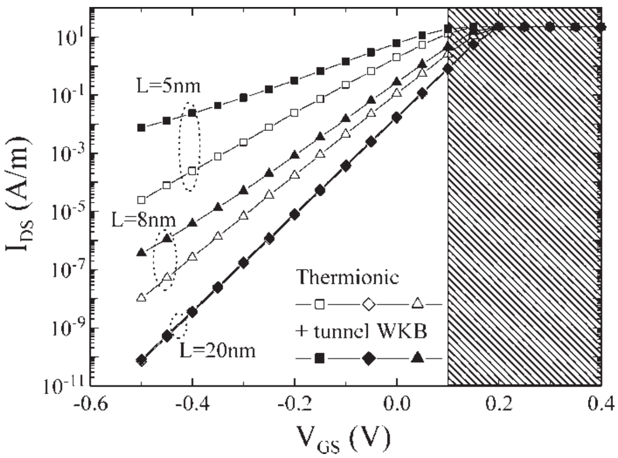

Figure 4. Subthreshold $I_{DS}(V_{GS})$ characteristics calculated with the analytical model when considering the WKB tunneling component in the ballistic current or not. Device parameters are the same as in figure 2.

tunneling contribution in the ballistic current or not two series of curves have been plotted. These results highlight the dramatic impact of the source-to-drain tunneling on the subthreshold slope and also on the I_{off} current. In this subthreshold regime, the carrier transmission by thermionic emission is reduced or even suppressed due to the high channel barrier; consequently, when the channel length decreases the tunneling becomes dominant and constitutes the main physical phenomenon limiting the devices scaling, typically below channel lengths of $\sim 10\,\mathrm{nm}$.

Model improvement: numerical aspects

Finally, we report here how the present approach can be further transformed from an analytical to a compact model and then extended to all the device operation regimes. In this later approach, equation (3) is numerically solved using a 1D finite difference scheme with a uniform mesh Δx. The distribution of electrons in the channel $n(x)$ can be also added in the second hand of equation (3) (assuming a linear electron quasi-Fermi level profile in the channel for low V_{DS} operation) which can be rewritten under the form:

$$\frac{\psi_{i+1} + \psi_{i-1} - 2\psi_i}{2\Delta x^2} - \frac{2C_{ox}}{\varepsilon_{Si} t_{Si}}\psi_i = \frac{1}{\varepsilon_{Si} t_{Si}}\left[qN_A t_{Si} - 2C_{ox}(V_{GS} - V_{FB} - \phi_F) + qt_{Si} n(x)\right] \quad (24)$$

A similar equation must also be considered to extend the simulation domain to source and drain regions, allowing us to take into account the electric field penetration in the reservoirs. After solving equation (24), the resulting potential profile $\psi_i(x_i)$ can be used to perform a more accurate calculation of the barrier transparency, using the transfer matrix (TM) method.[5] Such a numerical approach is interesting since a corrected transparency from the effect of carrier reflections on the barrier is obtained. In this case, because a unit transparency is not always achieved for carrier energies above $E_{1,max}$, the total ballistic current (thermionic + tunneling) must be evaluated over the whole energy range as follows:

$$I_{DS} = \frac{2q}{\pi^2 \hbar} \int_{-\infty}^{+\infty} dk_z \times \int_0^{+\infty} \left[f(E, E_{FS}) - f(E, E_{FD})\right] T_{TM}(E_x)\, dE_x \quad (25)$$

On a computational point-of-view, the calculation of the drain current per bias point with this approach takes less than one second on a desktop computer. Figure 5 compares $I_{DS}(V_{GS})$ characteristics obtained with the compact model and with the two transparency calculation methods. As expected, I_{DS} evaluated using the TM method is lower than the WKB current, due to carrier reflections on the barrier. Note that this phenomenon not only impacts I_{DS} in the subthreshold regime but also above threshold, due to the presence of a residual barrier in the channel near the source. The difference between the two currents, however, become negligible in the subthreshold region for "long" channels ($L = 20\,\mathrm{nm}$).

Conclusion

An analytical model for the subthreshold drain current in ultra-thin symmetric DG MOSFETs working in the ballistic regime is presented. The model is particularly well-adapted for ultra-short DG transistors in the decananometer scale since it accounts for the main physical phenomena related to these ultimate devices: 2D short-channel effects, quantum vertical confinement as well as carrier transmission by both thermionic emission

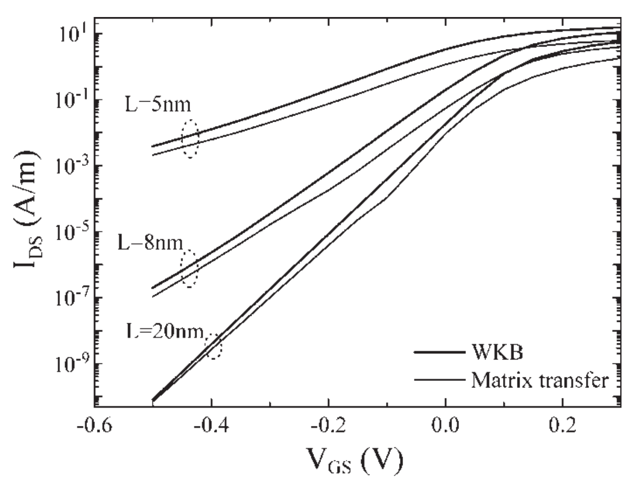

Figure 5. $I_{DS}(V_{GS})$ characteristics calculated with the compact model using two different evaluations of the source-to-drain barrier transparency. Device parameters are the same as in figure 2.

and quantum tunneling through the source-to-drain barrier. The model is used to predict essential subthreshold parameters such as off-state drain current and subthreshold slope and can successfully be included in circuit models for the simulation of DG MOSFET-based ICs.

Acknowledgments

The authors would like to thank T. Skotnicki and S. Harrison (ST Central R&D, Crolles, France) for fruitful discussions. This work is partially supported by the French Ministry of Industry (RMNT project “CMOSDALI” n° 02M0878), by the European Commission (Network of Excellence “SINANO”, IST contract n°506844) and by the Centre National de la Recherche Scientifique (CNRS, PICS n° 1950).

References

[1] K. Natori. Ballistic metal-oxide-semiconductor field effect transistor. *J. Appl. Phys.*, **76**, 4879 (1994).

[2] A. Rahman, M.S. Lundstrom. A compact scattering model for the nanoscale double-gate MOSFET. *IEEE Trans. Electron Dev.*, **49**, 481 (2002).

[3] Y. Naveh, K.K. Likharev. Modeling of 10-nm-scale ballistic MOSFETs. *IEEE Electron Dev. Lett.*, **21**, 242 (2000).

[4] D.K. Ferry, S.M. Goodnick. *Tranport in Nanostructures*, Cambridge University Press, Cambridge (1997).

[5] C. Cohen-Tannoudji, B. Diu, F. Laloë. *Quantum Mechanic*, Hermann, Paris (1992).

[6] D. Munteanu, J.L. Autran. Two-dimensional modeling of quantum ballistic transport in double-gate SOI devices. *Solid-State Electron.*, **47**, 1219 (2003).

[7] J. Guo, M.S. Lundstrom. A computational study of thin body, double gate, Shottky barrier MOSFETs. *IEEE Trans. Electron Dev.*, **49**, 1897 (2002).